OCL 2026, 33, 22

https://doi.org/10.1051/ocl/2026012

OCL Oilseeds & fats Crops and Lipids

Available online at:
www.ocl-journal.org

RESEARCH ARTICLE OPEN ACCESS

Factors contributing to the variability in sunflower achene dehulling efficiency☆

Patrick Carré[1,*], Laurent Gervais[2], Marie Coque[3], Jean-Philippe Loison[4] and Vincent Jauvion[1]

[1] Terres Inovia (DTVG), 11 rue Gaspard Monge, 33610 Canéjan, France
[2] RAGT 2n, La Courtade Haute, F-81600 Rivières, France
[3] SOLTIS Research, Domaine de Sandreau, 31700, Mondonville, France
[4] ITERG, 11 rue Gaspard Monge, 33610 Canéjan, France

Received 7 August 2025 – Accepted 14 April 2026

Abstract – This study aims to identify the morphological and anatomical factors that influence the dehulling capacity of sunflower achenes, a critical issue for the oilseed industry. Four cultivars grown at two sites over two cultivation years were examined. The study is based on observations from transverse sections of achenes, enabling measurement of the area of the achenes, embryos, and pericarp, as well as the length of contact zones between the pericarp and the embryo. Calculations were used to evaluate pericarp thickness, filling rate, and contact rate. Dehulling capacity does not simply depend on achene size or oil content but rather results from a complex balance between pericarp rigidity (as determined by its thickness) and the presence of gaps or adhesion zones at the pericarp/embryo interface. Genetic factors influence pericarp thickness and the propensity for hull/kernel contact. Environmental conditions impact the supply of water at both the flowering and seed-filling stages. The flowering period is crucial for pericarp development, and water stress during this period results in thinner pericarps and smaller achenes that are more difficult to dehull. The filling rate increases when water needs during seed filling are met, whereas the contact zones depend on the interaction between water supplies during both stages. In summary, the findings validate the role of the hull/kernel interface in dehulling and provide fresh avenues for selecting varieties with superior technological quality in sunflower achenes.

Keywords: Sunflower / dehulling / anatomy

Résumé – Facteurs contribuant à la variabilité de l'aptitude au décorticage des akènes de tournesol. Cette étude vise à déterminer les facteurs morphologiques et anatomiques qui influencent l'aptitude au décorticage des akènes de tournesol, une problématique majeure pour l'industrie oléagineuse. Les auteurs ont étudié 4 cultivars issus de deux sites et deux années de culture. L'étude résulte d'observations de coupes transversales d'akènes ayant permis de mesurer l'aire des akènes, des embryons et du péricarpe ainsi que la longueur des zones de contact entre péricarpe et embryon. Par calcul, l'épaisseur du péricarpe, le taux de remplissage et le taux de contact ont été évalués. L'aptitude au décorticage ne dépend pas simplement de la taille de l'akène ou de la teneur en huile, mais résulte d'un équilibre complexe entre la rigidité du péricarpe (fonction de son épaisseur) et la présence d'espaces ou de zones d'adhérence à l'interface coque/amande. L'effet génétique s'exprime au niveau de l'épaisseur du péricarpe et de la propension à former des contacts coque/amande. L'environnement intervient par la couverture des besoins en eau à la floraison et au remplissage. La période de floraison est clé pour le développement du péricarpe et un stress hydrique en cette période aboutit à des péricarpes plus fins et des akènes moins volumineux plus difficiles à décortiquer. Le taux de remplissage augmente lorsque les besoins en eau au remplissage sont satisfaits tandis que les zones de contacts dépendent de l'interaction entre le niveau de couverture des besoins en eau aux deux périodes. En conclusion, cette étude a confirmé l'importance de l'interface coque/amande pour le

☆ Contribution to the Topical Issue: "Technological challenges in oilseed crushing and refining / Défis technologiques de la trituration et du raffinage des oléagineux".

*Corresponding author: p.carre@terresinovia.fr

décorticage et donne de nouvelles perspectives pour la sélection variétale en vue d'améliorer la qualité technologique des graines de tournesol.

Mots clé : Tournesol / décorticage / anatomie

Highlights

- Close pericarp/embryo contact is likely to cause hull adherence in sunflower dehulling.
- Water stress at the flowering stage results in thinner pericarp.
- Genetic factors influence pericarp thickness and the tendency to form pericarp–embryo contacts.
- The interaction between water availability at flowering and seed filling stages determines the extent of hull–kernel contacts.

1 Introduction

Dehulling sunflower achenes prior to crushing is a key technological step to upgrade both meal and oil quality, with direct economic consequences for crushing plants and feed manufacturers. Removing fibrous hulls allows a substantial increase in protein concentration and amino acid digestibility in sunflower meal, which is essential for formulating rations for monogastric species such as poultry that require concentrated nutrients. Because dehulling remains limited, sunflower meal protein content is typically around 35%, while complete dehulling could yield protein levels approaching those of soybean meal. In parallel, removing hulls reduces the load of waxes and colored pigments in crude oil and limits the abrasive effect of silica-rich hulls on mechanical presses, thereby decreasing specific energy consumption and equipment wear, provided that adapted pressing conditions are implemented (Nolasco *et al.*, 2002; Rousseau *et al.*, 2025). Improved dehulling efficiency thus simultaneously increases crushing capacity, reduces oil losses in the hull fraction, and upgrades the commercial value of both meal and oil.

Yet, despite this technological and economic importance, the reasons why sunflower dehulls poorly in many industrial situations remain only partly understood. A general decline in dehulling efficiency has been reported and is often attributed to genetic progress for higher oil content combined with lower thousand seed weight (TSW), but a synthesis of published data shows only moderate correlations between dehulling rate and oil content, TSW, or bulk density (Carré *et al.*, 2025). The effect of water has been investigated by several authors (Gupta and Das, 2000; Khodabakhshian *et al.*, 2011; Saha *et al.*, 2012; Manikantan *et al.*, 2014). It increases the elasticity of both pericarp and kernel, thereby enhancing their ability to absorb impact energy and reducing their brittleness (Nolasco *et al.*, 2002; De Figueiredo *et al.*, 2011).

Other studies have examined hull structural traits and their genetic or environmental determinants. Morrison *et al.* (1981) showed that high-oil genotypes can exhibit contrasting hull structures, suggesting that hullability and oil concentration are not necessarily antagonistic. Reduced achene size has been associated with poorer dehulling aptitude (Dedio and Dorrell, 1989), but size alone is not decisive, since within small-seeded material some striped-hull cultivars remain easy to dehull (De Figueiredo *et al.*, 2011). Numerical modelling has further highlighted structural weaknesses at parenchyma–sclerenchyma junctions, underlining the role of internal pericarp architecture in impact resistance (Hernández and Belles, 2004). Environmental conditions during reproductive development also modulate dehulling aptitude: high-yield, high-oil plots may show poorer hullability (Di Leo *et al.*, 2004); reduced radiation during fruit filling can lower oil concentration without affecting final kernel size (Izquierdo *et al.*, 2008); and shading during pericarp formation reduces lignification and cellulose density in sclerenchyma, alters the pattern of parenchyma rays, and decreases dehulling efficiency without changing achene volume or density (Beauguillaume, 1994; Lindström *et al.*, 2006, 2007, 2022).

Genetic progress for higher oil content in sunflower has frequently been associated with thinner, less lignified pericarps; smaller achenes; and a reduced void between hull and kernel, which have been proposed as contributing to poorer dehulling (Morrison *et al.*, 1981; Mantese *et al.*, 2006; Lindström *et al.*, 2022). Because the pericarp completes its growth before embryo maturation, high-oil cultivars with shorter pericarp growth phases tend to limit the hull-to-kernel ratio and favor embryo expansion and lipid accumulation, thereby increasing the filling rate and potentially reducing the internal air gap (Mantese *et al.*, 2006).

The present work was motivated by repeated observations of hull–kernel adhesion in poorly hullable industrial lots, a phenomenon rarely analyzed explicitly in the dehulling literature despite its potential impact on hull extraction rate. Building on a previous study that related dehulling efficiency to water availability at flowering and during fruit filling (Carré *et al.*, 2025), the working hypothesis here is that dehulling aptitude depends not only on achene size, oil content, and global pericarp rigidity, but also on the geometry of the pericarp–embryo interface and the extent of close contact zones that may generate adhesion. Specifically, sunflower dehulling is expected to result from a balance between pericarp elasticity governed by thickness, sclerenchyma structure, and lignification and the degree of hull–kernel separation determined by filling rate and interface configuration. Using achenes from four commercial hybrids grown at two sites over two years, this study therefore aims to quantify pericarp thickness, achene filling rate, and the proportion of hull–kernel contact and to relate these morpho-anatomical traits to dehulling efficiency measured with a standardized centrifugal impactor test (Di Leo *et al.*, 2004; Dauguet *et al.*, 2016). The objective is to determine whether these interface-related traits, together with pericarp elasticity proxies, explain dehulling variability better than conventional bulk parameters and to provide more precise breeding and crop-management targets for improving dehulling efficiency and, ultimately, the economic value of sunflower products.

2 Material and methods

2.1 Origin of the achene studied

Four cultivars were chosen from the 30 commercial sunflower hybrids evaluated in the Carré *et al.* (2025) study: the first two exhibited low dehulling performance, while the other two showed greater dehullability. For confidentiality reasons, the identities of the cultivars cannot be disclosed. These varieties originated from four environments represented by two cultivation sites (Azay and Cham) and two growing seasons (2021 and 2022). The Azay 21 and 22 sites were approximately 2 km apart, while the two Cham trials were located 300 m apart and benefited from similar soil types. The 2021 season featured more favorable crop water satisfaction (72%) compared with 2022 (26%), calculated as the ratio of cumulative precipitation plus irrigation to potential evapotranspiration.

All plots were harvested on the same day. The experimental design included two replicates per hybrid. Row spacing was 0.6 m, with sowing densities between 73,000 and 75,000 seeds per hectare. Nitrogen and irrigation followed local best practices and differed between sites and years, as detailed in (Carré *et al.*, 2025). The Cham site received irrigation for emergence in both years (20 mm in 2021 and 50 mm in 2022), with an additional 30 mm irrigation applied on 12 July 2022. During the season, flowering onset dates were recorded for all plots. Harvested plot areas ranged from 12 to 18 m^2.

2.2 Dehulling ability measurements

Sunflower achene dehulling aptitude was measured using the method described by Dauguet *et al.* (2015). Approximately 80 g of achenes were conditioned for a minimum of two weeks at ambient temperature in a chamber with an ammonium nitrate-saturated aqueous solution, maintaining relative humidity between 62.5% and 65.5% at 20–25°C (Winston and Bates, 1960) to equilibrate moisture content. The achenes were then divided into four 20-g aliquots, with three aliquots used for dehulling aptitude measurement and one for moisture content determination.

The dehulling test employed a centrifugal impactor consisting of a 200-mm diameter disk with radial channels rotating at 2000 rpm. Three successive impacts were applied to each sample. The resulting fragmented material underwent separation in two stages: first through a 2-mm rotary sieve to isolate the “fines” fraction, followed by air-column separation to partition “hulls” from the “dehulled” fraction containing kernels, intact achenes, and broken achenes retaining partial pericarp. The three fractions were weighed using a balance accurate to 0.01 g. Moisture content was determined gravimetrically by measuring mass loss after 15 h at 103°C.

Dehulling efficiency was defined as the hull extraction rate (EH), *i.e.*, the mass percentage of recovered hulls relative to the initial achene mass. In commercial hybrids, this indicator was shown by Dauguet *et al.* (2015) to be strongly correlated with the dehulling rate expressed as EH divided by hull content.

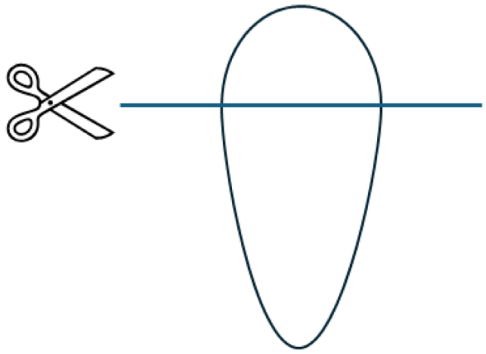

Fig. 1. Orientation of the section made for anatomical observations.

2.3 Morpho-anatomical study of achenes (dataset with each individual observation)

Achenes were transversely sectioned using a razor blade at approximately 25% of the distance from the widest end (Fig. 1). These sections were photographed under a magnifying loupe at 200× magnification. The resulting images were analyzed using ImageJ software. Figure 2 presents the manual measurements, which were performed to determine the cross-sectional area (A1) and perimeter (P1) of the achene, the area (A2) and perimeter (P2) defined by the inner pericarp limit, the area and perimeter of the embryo (A3, P3), and the length and number of zones exhibiting close contact between the embryo and pericarp (Pc, Nc) (Fig. 2). The pericarp area (Aperic) was calculated by subtracting A2 from A1. Mean pericarp thickness (PrThick) was estimated by dividing the pericarp area by the inner perimeter (Aperic/P2). The void space (void) between the pericarp and embryo was derived by subtracting the embryo area from the inner pericarp area (A2 – A3). The contact length (Pc) was computed as the sum of all segments along the embryo perimeter where the embryo and pericarp were in direct contact. The achene filling ratio (RoF) was calculated as the embryo area divided by the inner pericarp area (A3/A2). Finally, the rate of contacts (RoC) was defined as the contact length divided by the embryo perimeter (Pc/P2) the figures 1 and 2 have disappeared.

These analyses have been carried out on a minimum of 30 achenes per sample.

2.4 Meteorological data

For each experimental site, meteorological data were obtained from the nearest Météo-France weather stations. The recorded variables included precipitation, maximum and minimum temperatures, sunshine duration (in hours), wind, and humidity. These data were used to estimate potential evapotranspiration, which reflects the water requirements of the plant canopy.

These records enabled calculation of cumulative precipitation and potential evapotranspiration, which were used to calculate the proportion of crop water requirements met by rainfall. These coverage rates were calculated for the entire crop cycle (from sowing to harvest), for the flowering period (considering the week before and after flowering, WRC1), and for the late cycle (from 15 days after the start of flowering to

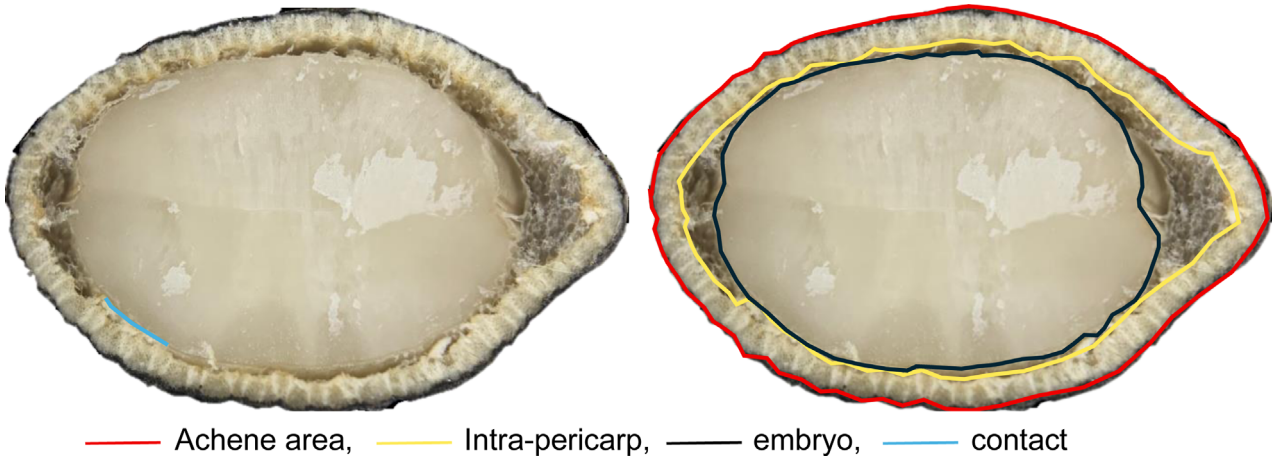

Fig. 2. Example images used for the analysis, featuring contour delineation employed to measure areas, perimeters, and the length of contact zones between the pericarp and embryo.

Table 1. Correlation matrix of dimensional parameters.

	A1	A2	A3	P1	P2	P3	Void	Aperic	Pc	PrThick	RoC	RoF
A1	1.000											
A2	0.991	1.000										
A3	0.905	0.923	1.000									
P1	0.967	0.950	0.872	1.000								
P2	0.968	0.961	0.882	0.989	1.000							
P3	0.850	0.860	0.894	0.836	0.835	1.000						
Void	0.554	0.538	0.171	0.522	0.528	0.243	1.000					
Aperic	0.904	0.839	0.736	0.899	0.868	0.714	0.534	1.000				
Pc	0.085	0.102	0.254	0.049	0.075	0.166	-0.294	0.020	1.000			
PrThick	0.758	0.668	0.578	0.766	0.707	0.581	0.443	0.953	-0.018	1.000		
RoC	-0.091	-0.076	0.051	-0.127	-0.102	-0.040	-0.305	-0.130	0.965	-0.142	1.000	
RoF	-0.238	-0.216	0.152	-0.233	-0.232	0.048	-0.885	-0.278	0.382	-0.267	0.343	1.000

Abbreviations: A1: surface of the achenes, A2: surface delimited by the inner edge of the pericarp, A3: surface of the embryo, P1–3 perimeters, Void: A2 – A3, Aperic: A1 – A2, Pc: length of the contact lines, PrThick: pericarp thickness, RoC: rate of contact Pc/P3, RoF: rate of filling (A2 − A3)/A2.

harvest, WRC2). In cases where irrigation was applied, water inputs were added to precipitation totals. These data were analyzed in a previous article (Carré *et al.*, 2025) and demonstrated that the percentage of extracted hulls could be predicted using two main variables: the proportion of crop water requirements met during flowering and the proportion of crop water requirements met during the achene filling period. These are the only variables retained for the present study.

2.5 Statistical analysis

Statistical analyses were performed using R and RStudio, version R 4.5.0 (2025-04-11 ucrt) R Core Team (2025).

3 Results

3.1 Raw morpho-anatomical observation data

Table 1 presents the correlation matrix for dimensional variables across the complete dataset (n = 544). Achene area (A1) and intra-pericarp area (A2) are almost perfectly correlated (r = 0.99), while the correlation between embryo and achene area remains strong but slightly lower (A1 × A3, r = 0.90), indicating variability in void space between hull and kernel. Void quantity is positively related to achene size (r = 0.55) but only weakly to embryo surface (r = 0.17). Perimeter–area relationships are strongly correlated for all structures, except for A3 × P3 (r = 0.89), reflecting greater embryo shape variability.

Supplementary material provides representative images for each variety and environment, using achenes with A1, A2, and A3 closest to lot means, which illustrates the within-variety morphological plasticity, notably the pronounced reduction in pericarp thickness in V01 and V04 at Azay22 compared with Cham21.

Void is more strongly correlated with A1 than with A3, suggesting that larger achenes more readily develop interstitial space, whereas kernel size is a poor predictor of this variable. Thus, achene and embryo areas are highly correlated (r = 0.905), but not perfectly, allowing substantial variability in hull–kernel interspace. Neither A1 nor A3 alone accurately

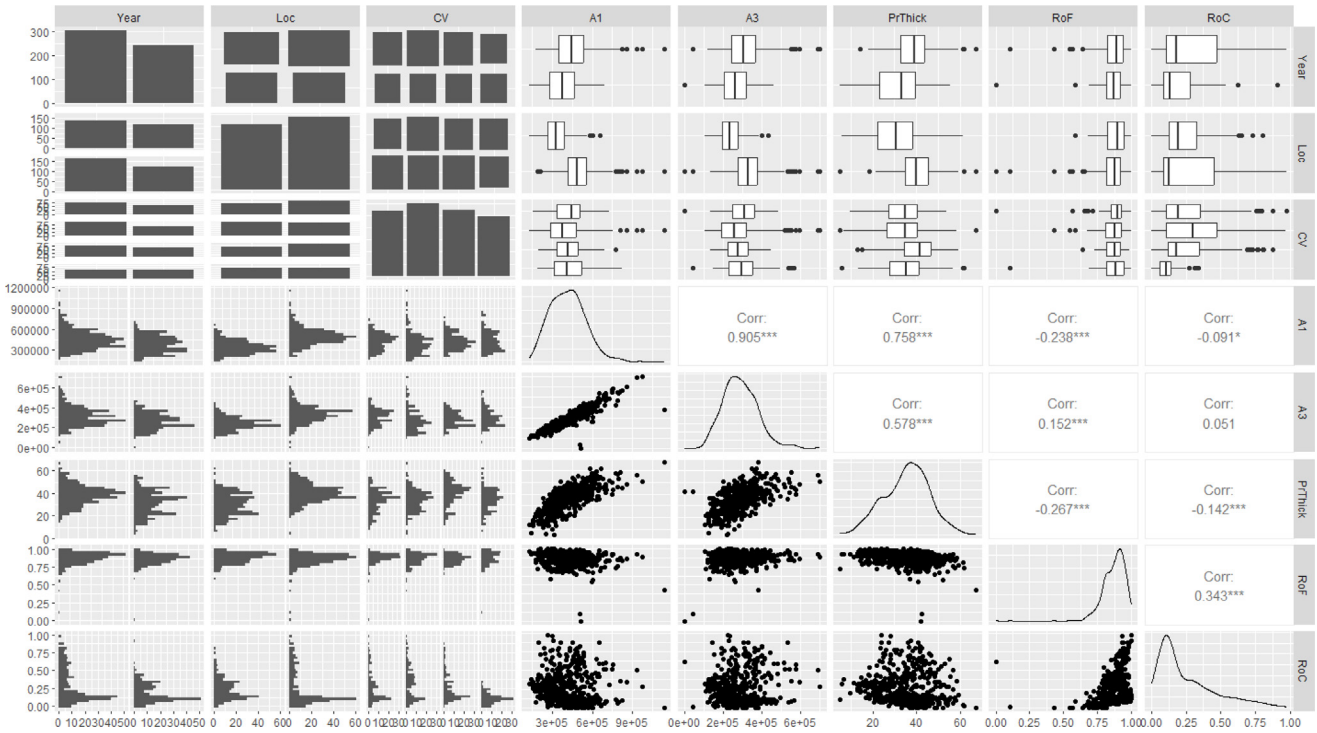

Fig. 3. Overview of the dispersion of the results of morpho-anatomic characterization of individual achenes. Loc: trial sites, CV: cultivar, A1: surface of achenes, A3: surface of the embryos, PrThick: thickness of pericarps, RoF: rate of filling, RoC: rate of contacts. The nine cells in the upper left panel give the number of observations for each combination of years (2021 and 2022), locations (Azay and Cham), and cultivar (V01, V04, V26, and V27). The upper right panel shows boxplots for each level of the variable considered. The lower left panel displays frequency histograms of the continuous variables for each level of the fixed factors, and the lower right panel shows pairwise scatterplots and correlation coefficients with significance codes: *** for $P < 0.001$, ** for $P < 0.01$, and * for $P < 0.05$. The diagonal of the correlation matrix shows the distribution curve of the data for each continuous variable.

predicts void and, even less, the filling rate (RoF). Pericarp thickness (PrThick) is moderately correlated with A1 (r = 0.76), indicating that thickness is not determined solely by achene size. Contact length (Pc) is only weakly correlated with filling rate (r = 0.38), a result whose interpretation will be revisited in relation to varietal effects. RoF is strongly but not perfectly related to void (r = −0.88), as it integrates both embryo expansion and cavity size, while RoC is tightly linked to Pc (r = 0.96).

Figure 3 summarizes the relationships between the main variables. Given the very high correlations between A1 and A2 and between P1 and P2, A1 and A3 were retained to represent size effects, whereas PrThick, RoF, and RoC were used to describe key dimensional traits. Sample sizes are balanced across treatments, always exceeding 30 observations, with slightly more achenes measured in 2021 than in 2022 and a somewhat larger sample for V04.

Distributions of A1 and A3 are asymmetric, mainly due to site effects, with a low frequency of very large achenes and a small number of poorly filled embryos, likely corresponding to nearly empty fruits. PrThick shows mild asymmetry but remains the most centered variable. RoF displays very few values below 0.75, with two modes around 0.82 and 0.91. RoC is markedly non-normal, with a main mode at 0.11 and a long right tail up to 1.

Table 2 reports F-values and significance levels for cultivar (CV), year, location (Loc), and interactions, using the model:

– Variable = CV + Year + Loc + Year × Loc + CV × Year + CV × Loc + CV × Year × Loc + intercept.

In the lower part of the table, the percentages of variance explained by each of these factors are shown.

Residual variance exceeds 50% for all variables, highlighting strong within-plot heterogeneity, but sample sizes remain sufficient to detect factor effects. Achene size (A1) is mainly driven by location (30% of variance) and year (8%), with a small yet significant cultivar contribution (0.7%) through interactions. Similar patterns are observed for embryo area. For PrThick, genetic effects are highly significant (6.2%), alongside year (11.2%) and especially location (19.7%), with only the year × location interaction significant, indicating that the varietal effect on thickness is stable across environments. RoF is poorly explained, with only location and the Loc×CV interaction contributing. By contrast, RoC is chiefly affected by the year×location interaction (18% of variance), followed by genetic (13.4%) and year effects (5.7%), while the main location effect remains limited.

3.2 Mean values of morpho-anatomical characteristics and extracted hull yield

Because both the anatomical observations and the dehulling test are destructive, dehulling aptitude could not

Table 2. Fisher's *F*-values and the percentage of variance accounted for by the factors cultivar (CV), year, location, and their interactions.

	F-value				
	A1	A3	PrThick	RoF	RoC
CV	2.3.	4 **	18.9 ***	0.6	45.4 ***
Year	75.8 ***	73 ***	103.1 ***	2.5	57.6 ***
Loc	290 ***	230.8 ***	182.4 ***	13.6 ***	2.7.
Year:Loc	0.4	0.2	34.6 ***	0.5	182 ***
CV:Year	6.5 ***	10.7 ***	1.7	0.2	16.3 ***
CV:Loc	7.5 ***	17.1 ***	1.9	5.4 **	4.7 **
CV:Year:Loc	4.6 **	5.1 **	3 *	1.9	14.4 ***
			Variance (SS type I)		
CV	0.7%	1.3%	6.2%	0.3%	13.4%
Year	7.9%	7.7%	11.2%	0.4%	5.7%
Loc	30.3%	24.5%	19.7%	2.4%	0.3%
Year:Loc	0.0%	0.0%	3.7%	0.1%	18.0%
CV:Year	2.0%	3.4%	0.6%	0.1%	4.8%
CV:Loc	2.4%	5.4%	0.6%	2.9%	1.4%
CV:Year:Loc	1.5%	1.6%	1.0%	1.0%	4.3%
Model	44.9%	44.0%	42.9%	7.3%	47.9%
residuals	55.1%	56.0%	57.1%	92.7%	52.1%

*Signif. codes: Pr(F) 0 '***' 0.001 '**' 0.01 '*' 0.05 '.' 0.1 ' ' 1*

be evaluated at the individual achene level. The analysis therefore relied on sample means, yielding a dataset of 16 observations (4 cultivars × 2 locations × 2 years).

3.2.1 Observation of the data by group of hullability

Figure 4 displays a series of boxplots representing the 16 available observations, grouped according to three dehulling aptitude classes (H−, H0, and H+). Initial classification by dehulling group reveals no overall significant differences in morphological traits. However, this lack of significance is largely driven by specific samples, such as cultivar V27, which exhibits low contact rates despite its group assignment. Similarly, the lack of significant differences in contact rate can be attributed to a V26 sample in the H+ group. Regarding achene filling rate, a notable difference is observed between the H− and H0 groups, suggesting that this criterion may have an effect that the limited statistical power of the experimental design fails to detect. The same applies to the effect of contact rate.

3.2.2 Observation of the data per cultivar

Figure 5 shows the distribution of morpho-anatomical variable observations for each cultivar across the four sites. Cultivars V01 and V04 exhibit lower dehulling performance than V26 and V27, as initially observed in the eight trial sites. A noteworthy characteristic of cultivar V26 is its thicker hulls (pericarp thickness), with a significant difference provided that the environment effect is included in the anova model (PrThick = Var + Env). Cultivar V27, on the other hand, shows a lower tendency than the other cultivars to develop contacts between the embryo and pericarp, although the Student–Newman–Keuls test falls below the threshold of statistical significance.

3.2.3 Results by environment

Figure 6 presents the same data but grouped according to the environment of origin of the achenes. This grouping reveals much clearer effects on morphological traits, although these do not translate into statistically significant differences in dehulling performance—likely because contrasting cultivars were systematically included in all four site-year combinations. The 22Azay trial is characterized by significantly thinner hulls compared with the other three trials. This difference is related to the reduced size of both the achenes and embryos in this environment. The filling rate is less dependent on environmental conditions, and within-group variability remains relatively high for this trait, although a significant difference is observed between 21Azay and 22Cham. Finally, the contact rate is strongly influenced by growing conditions, with 22Cham differing markedly from 21Cham for this trait.

3.3 Explaining the genetic and environmental effects by morpho-anatomic traits

3.3.1 Analysis of variance of the model EH = CV + Env

As a first approach, we must examine whether the variability in dehulling data can be explained by genetic and environmental factors through the analysis of variance using the model:

$$EH = CV + Env,$$

where EH is the percentage of hulls extracted after the dehulling test, CV is the cultivar effect, and Env is the combination of year and location. These results are presented in Table 3. Both genetic and environmental factors are individually significant at $Pr(F) < 0.01$. The genetic effect

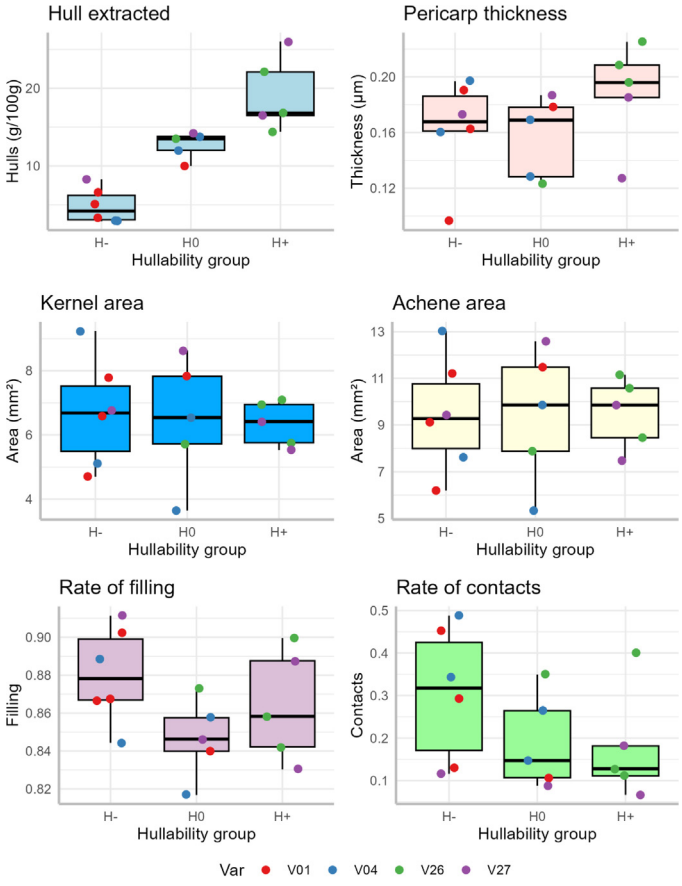

Fig. 4. Achene characterization according to dehulling groups (H−, low dehulling; H0, intermediate dehulling; H+, high dehulling) and cultivars. No significant differences were found between groups for any of the parameters, except for dehulling rate (by definition).

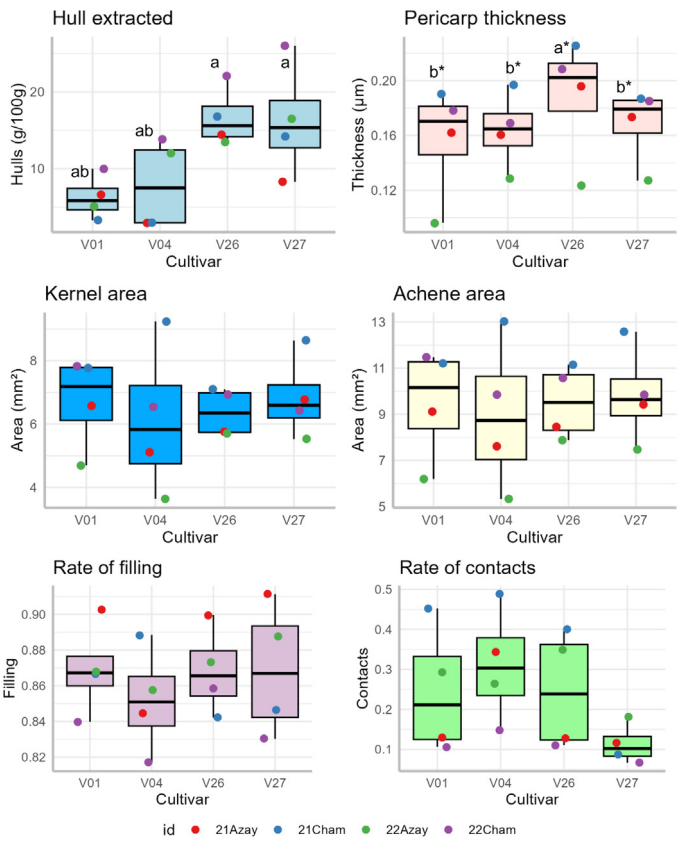

Fig. 5. Achene characterization by cultivar. No statistically significant differences were observed except for hull yield and pericarp thickness, provided that Azay 22 is excluded from the dataset. Groups of results with the same letter are not significantly different (Student–Newman–Keuls test).

accounts for 51.9% of the variance, compared with 33.8% for the environment.

The adjusted R^2 of the model is 0.76, while the probability of the associated Fisher's F is below the 1% threshold.

These results confirm that genetic effects account for a substantial share of the variation in dehulling efficiency.

3.3.2 Analysis of variance of the model EH = A1 + A3 + PrThick + RoC + RoF

Having confirmed the effects of genetic and environmental parameters, it is necessary to determine whether morpho-anatomical variables can account for the variability in EH. To this end, we performed stepwise multiple regression using the stepAIC() procedure in R, based on the bidirectional model:

$$EH = A1 + A3 + PrThick + RoC + RoF.$$

The procedure did not eliminate any variables, as removing any predictor did not improve the AIC value. Table 4 provides the model estimates, their standard errors, and the t-test evaluating the significance of each factor in the presence of all others.

The model has an adjusted R^2 of 0.656, and the F-test probability is less than 1%. However, the model is difficult to interpret because A1 and A3 are themselves highly correlated, and both are correlated with PrThick, which complicates the attribution of effects to individual predictors. The positive coefficient for A1 and the negative coefficient for A3 are consistent with the hypothesis that larger achenes are easier to dehull, especially if there is a void between the hull and the kernel. Nevertheless, under these circumstances, it is difficult to explain the fact that PrThick and RoF exhibit effects that contradict this hypothesis.

Removing PrThick from the model results in a substantial loss of predictive power, with an adjusted R^2 of 0.35 and a model no longer significant at the 5% threshold. Similarly, retaining PrThick while excluding A1 and A3 yields an adjusted R^2 of 0.31, with the model remaining significant at the 5% level.

3.3.3 Models integrating the cultivar effect

To better understand the environmental effect, we tested the same approach by forcing the inclusion of the cultivar factor into the model. Starting from the minimal model

$$EH = CV,$$

we allowed the algorithm to proceed up to the full model

$$EH = A1 + A2 + PrThick + RoF + RoC + CV.$$

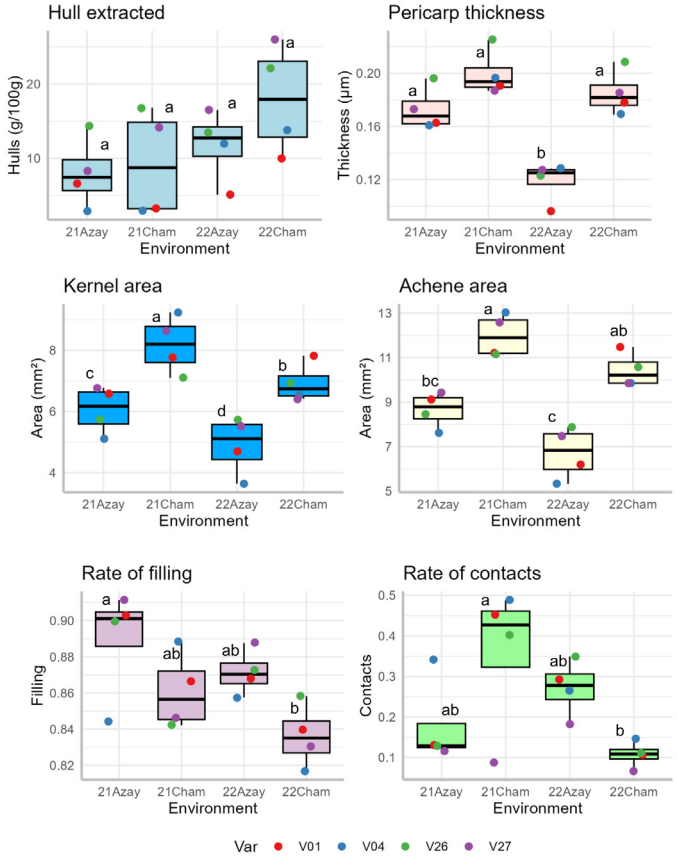

Fig. 6. Characterization of achenes according to their environment of origin and cultivar. Groups of results with the same letter are not significantly different (Student–Newman–Keuls test).

After two steps, the procedure converged onto the model EH = CV + RoF + RoC.

The model estimates and associated statistics are presented in Table 5.

The adjusted R^2 for Model 5 is 0.72, and the F-test probability is less than 1%. In this case, the environmental effect can clearly be interpreted as primarily influencing the filling rate and, to a lesser extent, the contact rate. For a better understanding of the role of these variables on the dehulling, we calculated their partial R^2 values. As a result, this calculation demonstrates that the rate of filling variable alone explains 14.9% of EH variability, while the rate of contact accounts for 8.8%, with 5.5% of variability stemming from the shared effect of both variables.

3.3.4 Models including the environmental effect

We adopted the same approach here by forcing the inclusion of the environmental factor into the model and allowing the algorithm to select the variables that account for the genetic effect.

Table 6 presents the model estimates and their associated probabilities. The model adjusted R^2 is 0.76, and the F-test probability is less than 1%. This model shows that PrThick and RoC are the main variables accounting for the varietal effect. The analysis of variance for the model indicates that pericarp thickness captures 32% of the variance and the contact rate accounts for 16%.

It means that within this dataset, the genetic effect manifests itself mainly by influencing the pericarp thickness and secondarily by the rate of contact between the hulls and the kernel.

3.4 Effects of water availability on morpho-anatomical parameters

Figure 7 shows the percentage of water requirements met during flowering and then during the seed-filling stage. In the 2021 growing season, water deficits were relatively similar at both sites during the filling period, while Azay experienced more pronounced water stress during flowering compared with Cham. In 2022, water deficits were diametrically opposed at the flowering stage, with Azay marked by severe water shortage, whereas Cham received abundant rainfall. In contrast, water stress during the filling phase was less pronounced at Azay than at Cham.

Finally, regarding the hull yield variable, only the 22Cham trial was found to be statistically different from the other three when considering all 30 cultivars studied.

3.4.1 Hull yield and water requirement satisfaction level

First, we tested the model
EH = CV + WRC1 + WRC2,

where WRC1 represents the percentage of water demand met during flowering and WRC2 the percentage met during the filling period.

Table 7 presents the analysis of variance for this model. The overall model has an adjusted R^2 of 0.78, and its F-test probability is below the 0.1% threshold.

In this scenario, the genetic effect accounts for 57% of the variability, water during the filling period for 18%, and water during flowering for 10%. As in our previous study involving 30 cultivars (Carré *et al.*, 2025), the effect of water availability during flowering on dehulling is positive, whereas adequate water supply during the filling period tends to reduce the hull yield.

3.4.2 Determinants of PrThick

To determine the best predictive model for PrThick, we employed stepwise multiple regression, forcing the inclusion of the cultivar variable (CV) and allowing the algorithm to select whether to include the WRC variables. The algorithm retained both WRC variables in addition to the varietal effect. Table 8 presents the analysis of variance for this model. The adjusted R^2 is 0.86, significant at the 0.1% threshold. The varietal effect on hull thickness appears rather modest, accounting for only 12% of the variance, whereas the percentage of water demand met during flowering predominates, capturing 46.5% of the variance, followed by water demand met during the filling period, which accounts for 32.5% of the variance.

According to the model estimates, the varietal effect is linked to the variety V26, which has significantly thicker hulls than the other three cultivars. The estimates for both WRCs (water requirement cover rates) are positive, meaning that higher water availability promotes greater hull thickness.

Table 3. ANOVA for the model EH = CV + Env.

	Df	Sum Sq	Mean Sq	*F*-value	Pr(>*F*)		% variance
CV	3	358.52	119.506	10.8866	0.002376	**	51.9%
Env	3	233.27	77.757	7.0835	0.009612	**	33.8%
Residuals	9	98.8	10.977				14.3%

Table 4. Estimates values of the model EH = A1 + A3 + PrThick + ROC + RoF selected by the stepAIC procedure.

	Estimate	Std.error	*t*-value	Pr(>|*t*|)	
(Intercept)	−378.295	135.208	−2.798	0.01886	*
A1	66.52	19.46	3.418	0.00657	**
A3	−87.173	25.052	−3.48	0.00593	**
PrThick	−717.636	237.973	−3.016	0.01299	*
RoC	−16.193	7.745	−2.091	0.06305	.
RoF	526.016	176.811	2.975	0.01393	*

Table 5. Estimates and associated statistics for the model EH = CV + RoF + RoC.

	Estimate	Std. Error	*t*-value	Pr(>|*t*|)	
(Intercept)	97.759	30.85	3.169	0.01001	*
VarV04	1.044	2.703	0.386	0.70742	
VarV26	10.385	2.555	4.065	0.00227	**
VarV27	7.687	2.763	2.782	0.01939	*
RoF	−100.423	35.798	−2.805	0.01863	*
RoC	−17.189	7.969	−2.157	0.05641	.

Table 6. Estimators and statistics associated with the model EH = Env + PrThick + RoC + RoF.

	Estimate	Std. Error	*t*-value	Pr(>|*t*|)	
(Intercept)	27.3022	40.4891	0.674	0.51706	
21Cham	−2.9752	3.5784	−0.831	0.42724	
22Azay	20.2281	4.005	5.051	0.00069	***
22Cham	0.7628	3.7513	0.203	0.84339	
PrThick	277.3128	60.5676	4.579	0.00133	**
RoC	−28.9978	8.557	−3.389	0.00801	**
RoF	−69.7467	46.8741	−1.488	0.17094	

3.4.3 Determinants of A1, achene surface area

As with shell thickness, the stepAIC() procedure was used to identify the most plausible polynomial model incorporating the three explanatory variables under consideration.

The selected model is expressed as:

A1 = CV + WRC1 + WRC2.

The results of the analysis of variance for this model are presented in Table 9. The varietal effect was found to be non-significant, whereas the effect of water requirement coverage at flowering explained 43.5% of the observed variability, and that during fruit filling accounted for 21.3%.

The adjusted R^2 is 0.50, while the unadjusted R^2 was 0.67, and the *F*-value is significant at the 5% threshold. The estimators are positive, suggesting that achene development responds favorably to adequate water requirement coverage, particularly during flowering. The constraint of forcing the CV variable into the model explains the relatively large discrepancy between the raw R^2 of the multiple regression and the adjusted R^2. When CV is removed from the model, the adjusted R^2 increases slightly to 0.56.

3.4.4 Determinants of A3, embryo surface area

Since the model obtained by forcing the inclusion of Cv in the multiple regression was not significant, we present here the analysis of variance (Table 10) of the model selected by the unconstrained stepAIC() procedure.

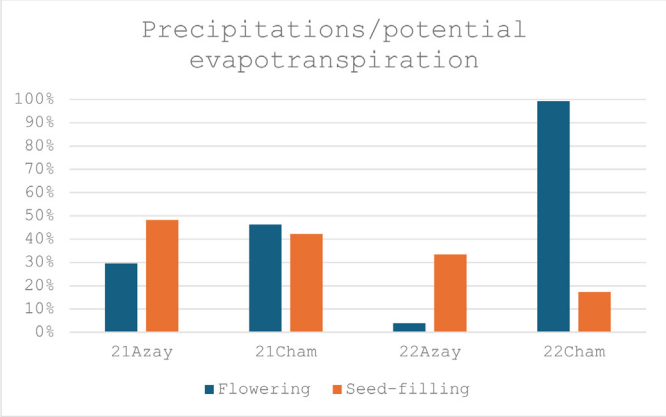

Fig. 7. Water requirement covering at flowering and seed-filling stages (WRC1, WRC2).

The adjusted R^2 of the model is 0.42, and the Fisher F-value indicates that it is significant at the 5% threshold. The water requirement coverage rate at flowering captures 27% of the variability compared with 23% for the fruit filling period.

3.4.5 Determinants of filling rate (RoF)

As previously observed, the selected model does not include the non-significant varietal factor. Table 11 shows that the WRC1 effect is significant at the 1% threshold, while the WRC2 effect is only significant at the 10% threshold.

The adjusted R^2 of the model is 0.50, and the probability associated with the model's F-value is significant at the 1% level. Thus, 41.7% of the variance is explained by water requirement coverage at flowering, while 15.2% is explained by coverage during fruit filling.

3.4.6 Determinants of contact rate (RoC)

On this occasion, the variable selection procedure retained the varietal factor as well as water requirement coverage during fruit filling. However, the model was not significant ($\Pr(F) = 0.167$). Table 12 shows that the varietal factor explains the largest proportion of the variance (28%), compared with 14% explained by water coverage during fruit filling.

The raw R^2 of the model is 0.42, while the adjusted R^2 is 0.21.

This weak level of significance is contradicted by the fact that the model RoC = Var + Env is significant at the 5% level and yields an adjusted R^2 of 0.60. For this reason, the WRC1 × WRC2 interaction was added to the procedure, which subsequently retained all proposed variables (Tab. 13).

The model exhibits an R^2 of 0.75 and an adjusted R^2 of 0.58, with a probability associated with the F-statistic of 0.023.

The WRC1 × WRC2 interaction is therefore determinant, as it accounts for 32% of the observed variability. The coefficients for both water requirement coverage rates have negative signs, whereas their interaction has a positive sign. To understand this interaction, let us construct a matrix in which we apply the model's coefficients to the minimum and maximum values of WRC to compute the predicted values of RoC. The respective coefficients for the intercept, WRC2, WRC1, and their interaction are 0.859, -1.80×10^{-2}, -9.86×10^{-3}, and $+3.33 \times 10^{-4}$.

Table 14 thus reveals a notably higher predicted contact rate (86%) when water stress occurs at flowering and water requirement coverage remains satisfactory during fruit filling, compared with a situation where water requirements are well met at both growth stages (71%). Furthermore, under water stress during fruit filling, the contact rate can remain relatively high (55%) if flowering is also subjected to stress, whereas it drops drastically (10%) when flowering does not experience water deficit.

4 Discussion

Before interpreting these results, it is important to note that statistical power was not homogeneous across analyses. Individual-level tests (correlations and ANOVA on dimensional traits) benefited from large within-treatment sample sizes (n = 544 achenes), whereas models fitted to treatment means (16 cultivar × environment combinations) had limited degrees of freedom. As a consequence, some non-significant effects, particularly for interactions or moderate genetic and environmental contrasts, should be regarded as inconclusive rather than as evidence of absence of effect, and the trends observed here would merit confirmation in larger, independent experiments.

In line with this limitation, our interpretation of how genetic and environmental effects are manifested through morpho-anatomical traits is exploratory and based on associations at the treatment mean level and should not be considered as a formal mediation analysis or proof of causal pathways.

4.1 Relevance of morpho-anatomical observations

Achenes exhibit substantial morpho-anatomical variability, partly due to their position on the capitulum and associated differences in assimilate supply. Centrally located achenes generally receive fewer assimilates than those in median or peripheral zones, and their later flowering makes them more exposed to abiotic stress. As a result, marked within-batch differences arise in the main morpho-anatomical traits, particularly filling rate, as illustrated in Figure 3 and Table 2. This variable shows especially high intra-batch variability compared with the other traits, reflecting heterogeneous assimilate transfer among achenes from the same lot.

The weak correlation between RoF and RoC (r = 0.34) is somewhat unexpected, since contact rate would intuitively be expected to increase with filing. The relationship is statistically detectable but remains modest.

Among the most difficult-to-dehull cultivars, average contact rates were lower than anticipated, and the V26 cultivar showed contact levels similar to poorly hullable ones. Supplementary sections illustrate that, in some achenes, the embryo integument closely follows pericarp irregularities, even where no visible void exists at the interface.

When present, these contact zones are generally limited to four in number, as the pericarp tends to be diamond-shaped

Table 7. Anova of the model EH = CV + WRC1 + WRC2.

	Df	Sum Sq	Mean Sq	*F*-value	Pr(>*F*)	
WRC1	1	70.55	70.547	7.0839	0.0238352	*
WRC2	1	127.16	127.16	12.7688	0.0050675	**
CV	3	393.29	131.097	13.1641	0.0008312	***
Residuals	10	99.59	9.959			

Table 8. Anova of the model PrThick = CV + WRC1 + WRC2.

	Df	Sum Sq	Mean Sq	*F*-value	Pr(>*F*)	
Var	3	0.0021868	0.0007289	4.3827	0.0325487	*
WRC1	1	0.0085065	0.0085065	51.146	3.10E-05	***
WRC2	1	0.0059373	0.0059373	35.6984	0.0001366	***
Residuals	10	0.0016632	0.0001663			

Table 9. Anova of the model A1 = CV + WRC1 + WRC2.

	Df	Sum Sq	Mean Sq	*F*-value	Pr(>*F*)	
CV	3	1.5821	0.5274	0.2196	0.880625	
WRC1	1	31.5967	31.5967	13.1542	0.004637	**
WRC2	1	15.4364	15.4364	6.4264	0.029614	*
Residuals	10	24.0202	2.402			

Table 10. Anova of the model A3 = WRC1 + WRC2.

	Df	Sum Sq	Mean Sq	*F*-value	Pr(>*F*)	
WRC1	1	8.4126	8.4126	6.9291	0.0207	*
WRC2	1	7.3272	7.3272	6.0351	0.02885	*
Residuals	13	15.7833	1.2141			

Table 11. Anova of the model RoF = WRC1 + WRC2.

	Df	Sum Sq	Mean Sq	*F*-value	Pr(>*F*)	
WRC1	1	0.0047789	0.0047789	12.5929	0.003566	**
WRC2	1	0.0017346	0.0017346	4.5708	0.05209	.
Residuals	13	0.0049334	0.0003795			

Table 12. Anova of the model RoC = CV + WRC2.

	Df	Sum Sq	Mean Sq	*F*-value	Pr(>*F*)
CV	3	0.082882	0.027627	1.7645	0.2119
WRC2	1	0.041251	0.041251	2.6346	0.1328
Residuals	11	0.172228	0.015657		

while the embryo is oval, resulting in the corners of the diamond being less frequently occupied. Figure S2 provides selected examples of these interfaces and illustrates how contact can be extremely close (as in image 3598, where protrusions of the pericarp appear almost absorbed by the embryo) or, conversely, limited to points of contact between

Table 13. Anova of the model RoC = CV + WRC2 + WRC1 + WRC1*WRC2.

	Df	Sum Sq	Mean Sq	*F*-value	Pr(>*F*)	
Cv	3	0.082882	0.027627	3.3065	0.071285	.
WRC2	1	0.041251	0.041251	4.937	0.053394	.
WRC1	1	0.002982	0.002982	0.3569	0.564961	
WRC2*WRC1	1	0.094048	0.094048	11.2559	0.008456	**

Table 14. Predicted values of RoC by the model RoC = WRC2 + WRC1 + WRC2*:WRC1.

WRC1/WRC2	17%	51%
1%	55%	86%
108%	10%	71%

procumbent vascular bundles (as in image 3087). Other images show comparatively large interspaces. These structural differences likely play a significant role in determining the dehulling performance of the achenes. When the protrusions of the pericarp, which correspond to the procumbent vascular bundles, penetrate the embryo's integument, it is plausible that this configuration reinforces the adhesion between these tissues, thereby increasing—or perhaps even preventing completely—the ability to dehull the achene.

Pericarp thickness is another anatomical trait influencing the efficiency of hull extraction. This effect is likely due to increased pericarp rigidity resulting from the development of lignified cell layers (Lindström *et al.*, 2022), which makes the pericarp more brittle. The role of pericarp rigidity in dehulling efficiency is further supported by observations from Gupta and Das (2000), who report that plasticity induced by moisture influences the mechanical resistance of shells under compression. The correlation between achene size and pericarp thickness may, however, confound the interpretation, as there is a positive relationship between these two parameters ($r = 0.758$), as well as between void quantity and achene size ($r = 0.554$), and between pericarp thickness and void quantity ($r = 0.443$). Therefore, it is conceivable that increased pericarp thickness simply reflects the presence of a greater void between the pericarp and embryo. The absence of a significant difference in pericarp thickness among the H+ achene group in Figure 4 is likely due to the inclusion within this group of a V27 sample from 22Azay, where water stress at flowering led to a marked reduction in pericarp development. Nonetheless, effective dehulling was still possible in these seeds, likely due to the capacity of V27 to avoid high contact rates between embryo and pericarp.

The scatterplot between filling rate and contact rate exhibits a triangular pattern (Fig. 3), indicating that while it is not possible to observe high filling rates associated with low contact rates, the converse is possible: low contact rates are compatible with both high and low filling rates. This observation accounts for the modest correlation coefficient between these variables ($r = 0.343$). It implies that although a high filling rate may be necessary for substantial contact rates, it is not sufficient on its own.

Pericarp thickness, filling rate, and the pericarp–embryo interface are three complementary morpho-anatomical traits that together account for a substantial part of the variability in sunflower dehulling efficiency, rather than being fully independent causal determinants. Our initial hypothesis—that the pericarp–embryo interface plays a significant role in achene dehullability—is supported by these observations, although this trait acts in combination with pericarp thickness, which itself correlates with achene size, as previously reported by Dedio and Dorell (1989). For effective dehulling, it is therefore necessary for achenes to be sufficiently large to allow substantial pericarp development, thereby creating space between the shell and the kernel. Satisfactory dehulling can be achieved even with a high filling rate, provided that the contact rate remains low.

4.2 Varietal effect

Table 6, which presents the model EH = Env + PrThick + RoC + RoF, shows that the varietal effect is conveyed mainly through pericarp thickness and contact rate, whereas Table 5 indicates that environmental effects act primarily via filling rate and, to a lesser extent, contact rate.

A noteworthy outcome is the comparison between EH prediction models: both the model including cultivar and environment (Table 3) and the model replacing cultivar with PrThick, RoF, and RoC (Table 6) have identical adjusted R^2 values (0.76). This strongly suggests that varietal differences in EH are largely driven by variation in pericarp thickness and in the propensity to develop high contact rates. Future breeding schemes could therefore aim at combining these favorable features while monitoring potential trade-offs with assimilate allocation to oil and protein deposition. These two axes are suitable candidates for future genetic dissection, for instance, through QTL mapping or genome-wide association studies, with the ultimate goal of developing molecular markers that track favorable combinations of pericarp thickness and interface architecture.

As shown in Figure 5, V26 is characterized by thicker pericarps, while V27 exhibits lower contact rates. This latter feature is particularly striking under the 21Cham conditions, where all other varieties show contact rates above 40%. Under 21Azay conditions, however, V27 reaches a filling rate close to 92%, and this high RoF limits hull extraction despite the favorable low contact rate.

Another striking result is the contrast between the key role of pericarp thickness in explaining genetic variation in hull extraction rate (Table 6) and the relatively modest share of its variance attributable to genetics (Table 8). In practice, inter-varietal differences in EH are mainly associated with pericarp thickness, whereas most of the variation in this trait arises from

environmental factors, especially water availability during flowering and fruit filling, with the varietal effect accounting for only about 12% of total variance.

This apparent paradox reflects the high plasticity of pericarp thickness: environmental conditions strongly modulate the trait, but small, stable genetic differences persist among cultivars. Even though the genetic component of PrThick is minor compared with environmental influences, these modest yet consistent differences between genotypes under comparable conditions are sufficient to generate a significant impact on dehulling efficiency. In other words, the genetic effect is expressed through a highly plastic trait whose total variance is largely environmentally driven, while its genotype-specific fraction still contributes meaningfully to varietal differences in EH.

4.3 Environmental effect

Our findings are consistent with those of Lindström *et al.* (2006, 2007, 2022), who observed that disruptions in plant function at the flowering stage can affect dehulling efficiency. These authors reported a decrease in hullability in response to shading at a stage when the pericarp has already reached its final size but has not yet completed cell division or lignification. Lindström and colleagues hypothesized that this effect causes the hulls to become more elastic, likely due to a lower density of lignified fibers, which allows them to absorb more of the energy from mechanical percussion during dehulling, reducing pericarp rupture. In the present study, water stress was shown to be a powerful factor in perturbing early achene development, potentially resulting in a reduction in total achene volume or in the development of the sclerenchyma responsible for pericarp rigidity. We had previously demonstrated that water requirement coverage at flowering and during fruit filling is the most predictive environmental factor for dehulling efficiency. In this study, using a smaller dataset, we were able to confirm that these two parameters remain significant in determining hull extraction rate (Table 7).

Our findings reinforce the link between environmental control of pericarp development and hullability, but in contrast to Lindström *et al.*'s focus on shading and lignification at flowering, we highlight the importance of the interface between the pericarp and embryo as an additional and complementary determinant of sunflower hulling efficiency. This advancement provides a more integrated explanation for the mechanisms responsible for poor hullability in sunflower achenes.

The influence of the seed-filling period on void fraction and kernel–hull rate of contacts is a key determinant of sunflower dehulling efficiency. Unfortunately, the conditions that favor agronomic productivity tend to impair dehulling performance. Agronomic room for maneuver therefore lies more in ensuring adequate water supply at flowering than in modifying the seed-filling period itself.

Concerning the possible influence of pericarp structure, specifically, the number and distribution of parenchymatous radial rays, as reported by Beauguillaume *et al.* and Lindström *et al.* on the stability of dehulling performance, our findings show that the adjusted R^2 values are perfectly aligned between the models EH = Cv + Env and EH = Env + PrThick + RoC + RoF. This suggests that, within our dataset, no additional factor is required to account for the varietal effect. However, we cannot rule out the possibility that expanding observations to new varieties might reveal a distinctive role for such factors in certain cultivars. Our results indicate that the dehulling efficiency of cultivars V26 and V27 stems from different characteristics: shell thickness for V26 and a propensity for low contact rates for V27. It is thus conceivable that pericarp structuring by radial rays may also contribute to differences in dehulling ability among commercial hybrids, although such an effect was not detected here.

5 Conclusion

Sunflower achene hullability in this study is mainly driven by three morpho-anatomical traits: pericarp thickness, the extent of key close contact zones at the pericarp–embryo interface, and achene filling rate. Together, these traits determine both hull rigidity and the ability of the pericarp to detach from the embryo under impact. Among easy-to-hull cultivars, one combined thicker hulls with good performance, while another showed a consistently low propensity to form tight contact zones, illustrating distinct but complementary ideotypes. Environmental effects act chiefly through water availability at flowering and during fruit filling, which strongly conditions the phenotypic expression of these genetic differences and confirms the high plasticity of hullability-related traits.

The experimental design, combining detailed morpho-anatomical measurements with explicit genetic and environmental analyses and multivariate modeling, clarifies how these traits relate to hull extraction rate and how they are shaped by genotype and environment. Limitations include the small number of hybrids, pronounced within-batch heterogeneity linked to achene plasticity, and the restricted set of site–year combinations, which resulted in only one environment with significantly different hullability. Nevertheless, the contrasted water regimes across the two sites and years were sufficient to reveal robust trends in the responses of pericarp thickness, filling rate, and contact rate.

These insights can now be translated into actionable breeding and crop management strategies. On the breeding side, pericarp thickness and interface architecture emerge as priority targets to improve hullability without unduly compromising kernel oil content, and their integration into imaging-based phenotyping and, ultimately, marker-assisted or genomic selection could accelerate the identification of favorable genotypes. On the agronomic side, a better understanding of genotype × environment interactions, particularly the sensitivity of pericarp development and hull–kernel interface traits to water stress at flowering, supports the design of irrigation strategies and the choice of sowing dates and earliness profiles that reduce the risk of poor hullability. In the context of recent harvests showing lower protein content in dehulled sunflower meals, such advances could help to anticipate fruit technological quality and to support the development of varieties that more reliably meet industrial requirements.

Acknowledgments

Artificial intelligence tools were used solely for improving English language expression and for assisting with R code generation. The AI was not involved in the study design, scientific writing, or data interpretation. All statistical analyses and results were independently verified and validated by the authors, who take full responsibility for the content.

Funding

The authors acknowledge the financial support of SOFIPROTEOL under the FSRSO Project PROTOUR.

Conflicts of interest

The authors declare no conflicts of interest.

Author contribution statement

Patrick Carré: investigations, original draft, reviewing & editing; Laurent Gervais: Fields trials, validation; Marie Coque: fields trials, validation; Jean-Philippe Loison: dehulling trials; Vincent Jauvion, achene analysis, reviewing & validation.

Supplementary material

Fig. S1 For each seed lot, an image of the achene whose dimensions are closest to the average achene of the batch. The proportions have been preserved.

Fig. S2 Pericarp embryo interface samples taken randomly (not representative of the average of each location × year × cultivar).

The Supplementary Material is available at http://www.ocl-journal.org/10.1051/ocl/2026012/olm.

References

Babic LJ, Radojcin M, Pavkov I, Babic M. 2012. The physical and compressive load properties of sunflower (*Helianthus annuus* L.) fruit. *Helia* 35: 95–112.

Beauguillaume A. 1994. Structure de l'akène de tournesol : influence sur l'aptitude au décorticage. PhD thesis, 2 vol., 149 p., 90, 1994TOU30002.

Bonnot T. 2016. Mechanical behaviour of hazelnut under compression loading: effect of moisture content. *J Food Eng* 168: 211–217. https://doi.org/10.1016/j.jfoodeng.2015.07.039

Carré P, Gervais L, Coque M, Loison L, Jauvion V. 2025. Sunflower achene hulling ability: impact of water availability and genetic. *OCL* (in press).

Chen P, Zhang L, Peng S. 2017. Mechanical properties of pecan shell biocomposites: effects of moisture and microstructure. *J Mater Sci* 52: 7357–7366. https://doi.org/10.1007/s10853-017-0977-x

Dauguet S, Labalette F, Fine F, Carré P, Merrien A, Palleau JP. 2016. Genetic impact on protein content and hullability of sunflower seeds, and on the quality of sunflower meal. *OCL* 23: D205.

De Figueiredo A, Baümler E, Riccobene IC, Nolasco SM. 2011. Moisture-dependent engineering properties of sunflower seeds with different structural characteristics. *J Food Eng* 102: 58–65.

Dedio W, Dorrell DG. 1989. Factors affecting the hullability and physical characteristics of sunflower achenes. *Can Inst Food Sci Technol J* 22: 143–146.

Di Leo MJ, Riccobene IC, Nolasco SM. 2004. Variability in dehulling ability of sunflower hybrids (*Helianthus annuus* L.) in Argentina. In: *Proc 16th Int Sunflower Conf*, pp. 591–595.

Gupta RK, Das SK. 2000. Fracture resistance of sunflower seed and kernel to compressive loading. *J Food Eng* 46: 1–8.

Hernández LF, Bellés PM. 2004. A 3-D finite element analysis of the sunflower (*Helianthus annuus* L.) fruit under impact: a useful approach for the understanding and improvement of its hullability. *WIT Trans Ecol Environ* 73.

Izquierdo NGA, Dosio GAA, Cantarero M, Luján J, Aguirrezábal LAN. 2008. Weight per fruit, oil concentration, and solar radiation intercepted during fruit filling in black hull and striped hull sunflower hybrids. *Crop Sci* 48: 688–699.

Khodabakhshian R, Emadi B, Abbaspour Fard MH, Saiedirad MH. 2011. Modeling the fracture resistance of sunflower seed and its kernel as a function of moisture content, variety, size and loading orientation. *Int J Food Eng* 7(3).

Lindström LI, Pellegrini CN, Aguirrezábal LAN, Hernández LF. 2006. Growth and development of sunflower fruits under shade during pre and early post-anthesis period. *Field Crops Res* 96: 151–159.

Lindström LI, Pellegrini CN, Hernández LF. 2007. Histological development of the sunflower fruit pericarp as affected by pre- and early post-anthesis canopy shading. *Field Crops Res* 103: 229–238.

Lindström LI, Franchini MC, Nolasco SM. 2022. Sunflower fruit hullability and structure as affected by genotype, environment and canopy shading. *Ann Appl Biol* 180: 338–347.

Manikantan MR, Selvam TA, Tarsem Chand TC, Rajiv Sharma RS, Sharma SR, Balakrishnan M. 2014. Fracture resistance behavior of sunflower (var. CO 2) seed and kernel under compression loading. *Madras Agric J* 101: 189–192.

Mantese AI, Medan D, Hall AJ. 2006. Achene structure, development and lipid accumulation in sunflower cultivars differing in oil content at maturity. *Ann Bot* 97: 999–1010.

Merrien A, Milan MJ. 1992. *Physiologie du tournesol*. Paris: CETIOM. ISBN 2-908645-31-9.

Morrison WH, Akin DE, Robertson JA. 1981. Open pollinated and hybrid sunflower seed structures that may affect processing for oil. *J Am Oil Chem Soc* 58: 969–972.

Nolasco SM, Riccobene IC, Fernandez MB. 2002. Dehulling of high oil sunflower seed grown in Argentina. In: *ASAE Annu Meet*, p. 1. American Society of Agricultural and Biological Engineers.

R Core Team (2025). R: A language and environment for statistical computing. R Foundation for Statistical Computing, Vienna, Austria.

Saha P, Manna S, Sen R, Roy D, Adhikari B. 2012. Durability of lignocellulosic fibers treated with vegetable oil–phenolic resin. *Carbohydr Polym* 87: 1628–1636. https://doi.org/10.1016/j.carbpol.2011.09.070

Silva CRS, Oliveira VL, Baskin CC. 2020. Biomechanics of seed coats as a defense against predators. *Ann Bot* 126: 781–790. https://doi.org/10.1093/aob/mcaa121

Winston PW, Bates DH. 1960. Saturated solutions for the control of humidity in biological research. *Ecology* 41: 232–237.

Zhang Y, Chen X, Wang S. 2018. Bioinspired core–shell composites with tunable mechanical properties. *ACS Appl Mater Interfaces* 10: 21335–21343. https://doi.org/10.1021/acsami.8b04451

Cite this article as: Carré P, Gervais L, Coque M, Loison J.-P., Jauvion V. 2026. Factors contributing to the variability in sunflower achene dehulling efficiency. *OCL* 33: 22. https://doi.org/10.1051/ocl/2026012